Dynamic expression of Id3 defines the stepwise differentiation of tissue-resident regulatory T cells

Jenna M. Sullivan[1,2], Barbara Höllbacher[1] and Daniel J. Campbell[1,2]*

[1]Immunology Program, Benaroya Research Institute, Seattle, WA 98101

[2]Department of Immunology, University of Washington School of Medicine, Seattle, WA 98195

*Corresponding Author: Daniel J. Campbell, Benaroya Research Institute, 1201 Ninth Avenue, Seattle, WA 98101-2795. E-mail address: campbell@benaroyaresearch.org

Abstract

Foxp3$^+$ regulatory T (T_R) cells are phenotypically and functionally diverse, and broadly distributed in lymphoid and non-lymphoid tissues. However, the molecular pathways guiding the differentiation of tissue-resident T_R populations have not been well defined. By regulating E-protein function, Id3 controls the differentiation of CD8$^+$ effector T cells and is essential for T_R maintenance and function. We show that dynamic expression of Id3 helps define three distinct T_R populations, Id3$^+$CD62L^{hi}CD44^{lo} central (c)T_R, Id3$^+$CD62L^{lo}CD44^{hi} effector (e)T_R and Id3$^-$ eT_R. Adoptive transfer experiments and transcriptome analysis support a stepwise model of differentiation from Id3$^+$ cT_R to Id3$^+$ eT_R to Id3$^-$ eT_R. Furthermore, Id3$^-$ eT_R have high expression of functional inhibitory markers and a transcriptional signature of tissue-resident T_R. Accordingly, Id3$^-$ eT_R are highly enriched in non-lymphoid organs, but virtually absent from blood and lymph. Thus, we propose that tissue-resident T_R develop in a multi-step process associated with Id3 downregulation.

Introduction

Several recent studies have highlighted the phenotypic and functional heterogeneity of regulatory T (T_R) cells during both steady state and inflammation (1-4). We and others have shown that at steady state in lymphoid organs T_R can be broadly divided by expression of CD44 and CD62L into distinct subsets which differ in their localization, dependence on IL-2, and extent of PI3K signaling (2, 5, 6). Moreover, CD44^{hi}CD62L^{lo} effector (e)T_R display diverse expression of transcription factors and chemokine receptors that promote their migration to inflamed tissues and their response to different types of inflammatory signals (1, 7). Accordingly, T_R found in nonlymphoid tissues have a distinct molecular profile that includes high expression of Gata3 and ST2 (the IL-33R) and are functionally equipped to suppress inflammation at barrier sites (8-10). Although these data highlight the anatomical, functional and molecular diversity of T_R, the pathways by which these T_R populations differentiate have not been completely defined.

The inhibitors of DNA binding (Id) proteins have been extensively studied in lymphocyte development (11, 12). Studies of CD8$^+$ effector T cells revealed that Id2 and Id3 are powerful transcriptional regulators of differentiation that are dynamically regulated during T cell activation and effector/memory T cell differentiation (13, 14). Through their regulation of E protein function, Id2 and Id3 help to control expression of genes essential for CD8$^+$ effector cell differentiation and survival such as *Tcf7*, *Tbx21*, *Bcl2* and *Klrg1* (15-17). Although less well studied, Id proteins have been shown to have essential roles in CD4$^+$ T cell function. For instance, Id2 and Id3 are essential for T_R maintenance and function, with T_R lacking both Id2 and Id3 having impaired proliferation and survival (18). In T_R, Id3 helps to stabilize Foxp3 through restriction of the E protein E47 and its downstream targets Spi-B and SOCS3 (19). However, Id3 expression is not uniform in T_R, and distinct populations of Id3$^+$ and Id3$^-$ have been identified (18, 20). In this study, we show that Id3 is dynamically regulated in T_R, and that progressive loss of Id3 correlates with the stepwise differentiation of highly-functional T_R population localized primarily in non-lymphoid tissues.

Results/Discussion

Id3 is dynamically expressed in T_R and regulated by TCR signaling

To examine Id3 expression in T_R we generated Id3-GFP x Foxp3-mRFP double reporter mice. In agreement with previously published reports, most CD4$^+$ T cells in spleen and lymph nodes (LNs) were Id3$^+$ (18, 20). However, we noted a subset of Id3$^-$ cells in both Foxp3$^+$ T_R and Foxp3$^-$ conventional CD4$^+$ T cell populations (Fig 1A). Within T_R, the Id3$^-$ population fell exclusively within the CD44^{hi} CD62L^{lo} eT_R compartment (5), whereas Id3$^+$ T_R were found in both the CD44^{lo} CD62L^{hi} central (c)T_R and eT_R compartments (Fig 1B). Thus, in secondary lymphoid

organs (SLOs) T_R can be divided into three distinct subsets based on Id3, CD62L and CD44 expression, Id3$^+$ cT_R, Id3$^+$ eT_R or Id3$^-$ eT_R. Within the Id3$^+$ T_R populations Id3$^+$ cT_R had higher Id3 expression than Id3$^+$ eT_R measured by GFP-MFI (Fig 1B), leading us to hypothesize that T_R may downregulate Id3 as they transition during their activation and differentiation from cT_R into eT_R. Indeed, Id3 expression can be downregulated by TCR signaling (18), and we observed a loss of Id3 expression in the T_R compartment correlating with the strength of TCR stimulation when cells were activated with different concentrations of platebound αCD3/28 for 48 hours (Fig 1C). To more precisely define the developmental relationship between these T_R subsets we sorted Id3$^+$ cT_R, Id3$^+$ eT_R or Id3$^-$ eT_R from spleen and LNs of reporter mice and transferred individual T_R populations into RAG1-deficient animals, and evaluated the phenotype and expansion of transferred T_R after 2 weeks. Transferred Id3$^+$ cT_R gave rise to all three subsets, with some cells retaining Id3 and CD62L expression but the majority converting into Id3$^-$ eT_R (Fig 1D). The bulk of Id3$^+$ eT_R downregulated Id3, with no cells regaining CD62L expression, whereas Id3$^-$ eT_R did not give rise to either of the other populations, indicating that these cells are likely a terminal differentiated population. Thus, Id3$^-$ eT_R appear to develop from Id3$^+$ cT_R in a stepwise manner during activation, with Id3$^+$ eT_R acting as an intermediate population.

Id3$^-$ eT_R express inhibitory markers and are highly suppressive

To explore the phenotypic and functional differences between these three subsets of T_R, we assessed expression of the T_R-associated surface markers on each population of splenic T_R. In agreement with previously published data, cT_R and eT_R showed distinct phenotypes, with eT_R having lower expression of the high affinity IL-2 receptor component CD25, but higher levels of the activation and functional surface markers ICOS, KLRG1, TIGIT, GITR and CTLA4 (Fig 2A) (5, 6). Moreover, within the eT_R compartment the Id3$^-$ T_R had higher expression of activation and inhibitory molecules than their Id3$^+$ T_R counterparts, and had the lowest expression of CD25. As our lab previously described (5), elevated expression of ICOS and diminished expression of CD25 suggests that Id3$^-$ eT_R are less dependent on IL-2 for their homeostatic maintenance, and instead likely rely on continued ICOS signaling. Additionally, increased expression of these T_R functional molecules correlated with enhanced *in vitro* suppressive activity of Id3$^-$ eT_R compared with either Id3$^+$ cT_R or Id3$^+$ eT_R (Fig 2B).

Transcriptional profiling highlights the stepwise differentiation of Id3$^-$ eT_R

To identify and compare their unique transcriptional profiles, we performed RNA-seq on sorted Id3$^+$ cT_R, Id3$^+$ eT_R and Id3$^-$ eT_R from spleen or LNs of Id3-GFP x Foxp3-mRFP reporter mice. Although there was little difference between LN and spleen samples, principle component analysis (PCA) showed that each of the three T_R populations were transcriptionally distinct (Fig 3A), and accordingly we identified 1,672 significantly differentially expressed (DE) genes between the three T_R populations (Fig 3B, Supplemental Table 1). The largest differences were found between Id3$^-$ eT_R and Id3$^+$ cT_R with 1,471 DE genes, whereas only 474 genes differed between Id3$^+$ and Id3$^-$ eT_R (Fig 3B). Interestingly among the DE genes we observed a reciprocal increase in Id2 expression as T_R lose Id3 (Fig 3C). This differential Id expression in T_R is similar to what occurs in CD8$^+$ T cells, which upregulate Id2 and downregulate Id3 while becoming activated and gaining effector function (13, 14). This suggests that as T_R downregulate Id3, the closely related Id2 may take over some of its functions while also driving a unique E-protein-dependent signature promoting eT_R development. Consistent with the stepwise differentiation model we propose for these populations, examination of the 300 most DE genes across the three T_R subsets (based on highest F-value) showed that both up and downregulated genes were generally expressed in a gradient fashion, with expression in Id3$^+$ eT_R falling between that of Id3$^+$ cT_R and Id3$^-$ eT_R (Fig 3D-E). Moreover, in accordance with our prior phenotypic analysis and their enhanced suppressive activity, Id3$^-$ eT_R showed elevated expression of known T_R function genes, including *Il10, Ctla4, Pdcd1, Tnfrsf4, Lag3 and Ebi3* (Fig 3F). Gene Ontology

(GO) term enrichment analysis of genes DE between Id3$^+$ eT$_R$ and Id3$^-$ eT$_R$ identified specific molecular pathways altered between these closely related populations (Fig 3G). The top six enriched categories all related to cytokine and chemokine receptor signaling, with Id3$^-$ eT$_R$ expressing high levels of receptors indicating that they can tune their activity in response to key inflammatory cytokines such as IL-1, IL-18, IL-23, and IL-25 (Fig 3H). Moreover, among the DE chemokine receptors, Id3$^-$ eT$_R$ had the highest expression of receptors that promote lymphocyte migration to inflamed tissues, such as *Ccr1, Ccr2, Ccr4, Ccr10, Cxcr3 and Cxcr6* (Fig 3H) (1) *.* Thus, Id3$^-$ eT$_R$ have a unique molecular profile indicative of their development from Id3$^+$ T$_R$ precursors, their elevated suppressive function and altered migratory capacity.

<u>Id3$^-$ T$_R$ are enriched and resident in non-lymphoid tissues</u>

In contrast to their elevated expression of inflammatory chemokine receptors, Id3$^-$ eT$_R$ had the lowest expression of *Ccr7* and *S1pr1* which function together to promote T$_R$ recirculation through SLOs (21) (Fig 3H). Additionally, expression of CD103 and CD69, which together act to retain tissue-resident memory T($_{RM}$) cells in non-lymphoid sites, was strongly enriched in Id3$^-$ eT$_R$, suggesting these cells may be tissue-resident (Fig 4A) (22, 23). Indeed, utilizing published gene signatures of CD8$^+$ T$_{RM}$ or circulating memory T cells (24), we found that the CD8$^+$ T$_{RM}$ signature gene set was enriched in Id3$^-$ eT$_R$ compared to either Id3$^+$ cT$_R$ or Id3$^+$ eT$_R$, whereas the circulating memory gene set was enriched in the Id3$^+$ T$_R$ populations (Fig 4B). Several groups have recently identified the ST2 (IL-33R)-Gata3 axis as a key determinant of T$_R$ residency and function in non-lymphoid tissues (8-10, 25, 26). Accordingly, Id3$^-$ eT$_R$ had the highest expression of all positively associated tissue T$_R$ genes such as *Il1rl1* (ST2), *Gata3*, *Areg*, *Irf4 and Rora*, whereas Id3$^+$ cT$_R$ had the lowest expression of these genes but high expression of negative regulators of tissue residence such as *Tcf7, Klf2* and *Lef1,* and Id3$^+$ eT$_R$ displayed intermediate expression for all of these genes (Fig 4C). Consistent with their T$_{RM}$-like transcriptional signature, Id3$^-$ eT$_R$ were a minority of T$_R$ in LNs and spleen, but their frequency dramatically increased in nonlymphoid tissues, where they highly expressed the T$_{RM}$ surface markers CD103 and CD69 (Fig 4D-F). Indeed, tissues such as the fat and skin contained almost exclusively Id3$^-$ eT$_R$. Of particular note Id3$^-$ eT$_R$ were rarest in the lymph and blood, indicating that Id3$^-$ eT$_R$ do not actively recirculate, but instead are retained as tissue-resident cells in non-lymphoid organs.

Despite significant interest in tissue-resident T$_R$, the mechanisms regulating their differentiation and distribution are still poorly defined. Our data show that T$_R$ can be subdivided based on Id3 expression and known markers of cT$_R$ and eT$_R$ into distinct populations, and we propose a stepwise model in which T$_R$ downregulate Id3 as they progressively gain effector function, tissue homing capacity and residency in non-lymphoid organs. Similarly, Li *et al.* recently proposed a stepwise model for the differentiation of T$_R$ in adipose tissue in which activation in the spleen allowed T$_R$ to migrate into the adipose tissue, where IL-33 signaling drove their terminal differentiation and functional specialization (26). High expression of co-stimulatory receptors such as ICOS and receptors for inflammatory cytokines would also allow Id3$^-$ eT$_R$ to respond to inflammatory signals that enhance Foxp3-mediated transcriptional repression and promote eT$_R$ differentiation and function (27), in part through activation of mTORC1 signaling (28). Although the direct role of Id3 downregulation in the functional differentiation of T$_R$ is still not established, our data highlight the complexity of tissue T$_R$ development, and identify novel molecular pathways that are modulated during their stepwise differentiation.

Materials and Methods

Mice

C57BL/6, RAG1-deficient and Foxp3-mRFP mice were purchased from The Jackson Laboratory. Id3-GFP mice were a generous gift from Ananda Goldrath (UCSD, La Jolla, California) and have been previously described (13, 15). All mice were bred and housed under the approval of the Institutional Animal Care and Use Committee of the Benaroya Research Institute.

Cell Isolation

Unless noted below, single cell suspensions isolated from tissues using manual disruption. PEC isolated by injecting sterile PBS into peritoneal cavity of euthanized mice, gentle disruption to dislodge cells and collection of injected PBS. IEL and LPL were isolated from pooled large and small intestine as previous described (29). Lymphocytes were further purified by resuspension in 44% Percoll™ (GE Healthcare) layered over 67% Percoll™ and spun at 2,800rpm for 20 mins. Lung and fat were finely minced, digested with 0.26U/mL Liberase TM (Roche) and 10U/mL DNAse (Sigma) for 1 hr at 37°C and filtered. For skin tissue, ears were processed as above with 0.14U/mL Liberase TM and 10U/mL DNAse. For lymph collection, mice were fed 20mL/kg 'Half and Half' by oral gavage and sacrificed 2-3 hrs later. Lymph collected from the cisterna chyli was directly stained for flow cytometry.

Flow cytometry

Single cells suspensions were stained with fixable Viability Dye eFluor 780 (eBiosciences) in PBS for 10 min at RT. Cells were stained with directly conjugated Abs in PBS with 0.5% BCS for 20 min at 4°C. Abs purchased from BioLegend: CD4 (RM4-5), TCRβ (H57-597), CD44 (IM7), CD62L (MEL-14), CD25 (PC61), ICOS (C398.4A), TIGIT (1G9), CTLA4 (UC10-4B9), GITR (DTA.1), CD69 (53-7.3). Abs purchased from eBiosciences: KLRG1 (2F1) and CD103 (2E7). Intracellular stains were performed using a FixPerm Kit (eBiosciences). Data acquired on an LSR II (BD Biosciences) and analyzed using FlowJo software (TreeStar).

In vitro assays

$CD4^+$ T cells isolated from spleen and LN using CD4 microbeads (Miltenyi). $1x10^6$ T cells cultured with platebound α-CD3 (2C11) and α-CD28 (37.51) from BioXcell at indicated concentrations for 48 hrs. *In vitro* T_R suppression assays were performed as previous described (30).

In vivo T_R transfer

Sorted T_R isolated from spleen and LN as described for RNA-seq. 100,000 sorted cells were injected retro-orbitally into RAG1-deficient hosts. Spleen, LN and blood of recipient mice collected two wks later and analyzed by flow cytometry.

Statistical Analysis

The *p* values were calculated by Prism software (GraphPad) using either an unpaired Student's *t* test or one way ANOVA as indicated. Values less than 0.05 were considered significant.

RNA-seq

$CD4^+$ T cells were isolated using CD4 microbreads (Miltenyi) from either peripheral LNs or spleens of 3 littermate Id3-GFP x Foxp3-mRFP mice. Cells were sorted based on viability, CD4, CD44, CD62L, Id3-GFP and Foxp3-mRFP expression on a FACs Aria II (BD Biosciences). 500 cells were sorted directly into SMART-Seq v4 Ultra Low Input RNA Kit (Takara) lysis buffer and protocol followed to produce cDNA. Library construction was performed using a modified protocol of the NexteraXT DNA sample preparation kit (Illumina). Dual-index, single-read

sequencing of pooled libraries was run on a HiSeq2500 sequencer (Illumina) with 58-base reads and an average depth of 8.6Mio reads per library. Base-calling and demultiplexing were performed automatically on BaseSpace (Illumina) to generate FASTQ files

RNAseq analysis

FASTQ files were processed to remove reads of zero length (fastq_trimmer v.1.0.0), remove adapter sequences (fastqmcf tool v.1.1.2) and perform quality trimming from both ends until a minimum base quality ≥ 30 (FASTQ quality trimmer tool v.1.0.0). Reads were aligned to the mouse reference genome (build NCBI37) with TopHat (v.1.4.0) and read counts per Ensembl gene ID were quantified with htseq-count (v.0.4.1). Quality metrics for the FASTQ and BAM/SAM files were generated with FastQC (v.0.11.3) and Picard (v.1.128). Processing of FASTQ and BAM/SAM files was executed on the Galaxy workflow platform of Globus genomics. Statistical analysis of gene expression was assessed in the R environment (v.3.4.4). All samples had > 90% of reads mapping to the reference genome and had a median CV coverage < 0.5. Ensembl Gene IDs were mapped to MGI gene symbols using biomaRt (v2.32.2). After filtering out lowly expressed transcripts and non-protein coding genes, we proceeded with 14011 genes. In order to normalize counts between samples, scaling factors for the raw library sizes were computed with edgeR::calcNormFactors (v.3.20.9). A linear model was fit to each gene with limma (v.3.34.9), making pairwise comparisons between the populations as contrasts (Id3pos_eTR-Id3pos_cTR, Id3neg_eTR-Id3pos_cTR, Id3neg_eTR-Id3pos_eTR). Differentially expressed genes were defined as adj.p.value < 0.05 and log2FC > 1. The log expression values were z-transformed by row in all heatmaps and the column dendrograms on top of the plots represents hierarchical clustering of Euclidean distances. Functional enrichment was assessed by taking the geneset of DE genes of $Id3^-$ eT_R vs $Id3^+$ eT_R and running goseq (v.1.30.0) to determine enrichment of gene ontology (GO) categories. Results were filtered for categories with a size < 500. Barcode plot for Trm and circulating memory signatures were generated with limma::barcodeplot and significance determined by rotation gene set tests with limma::roast.

Acknowledgements:

We thank A. Goldrath for Id3-GFP mice. K. Arumuganathan and T. Nguyen for help with flow cytometry and cell sorting. V. Gersuk and the BRI Genomics Core for running RNA-seq samples. And members of the Campbell lab for helpful discussions.

References

1. Campbell, D. J. 2015. Control of Regulatory T Cell Migration, Function, and Homeostasis. *J Immunol* 195: 2507-2513.
2. S., S. K., S. Shivani, S. J. Michael, and C. D. J. 2014. Regulatory T-cell homeostasis: steady-state maintenance and modulation during inflammation. *Immunological Reviews* 259: 40-59.
3. Dominguez-Villar, M., and D. A. Hafler. 2018. Regulatory T cells in autoimmune disease. *Nat Immunol*.
4. Josefowicz, S. Z., L. F. Lu, and A. Y. Rudensky. 2012. Regulatory T cells: mechanisms of differentiation and function. *Annu Rev Immunol* 30: 531-564.
5. Smigiel, K. S., E. Richards, S. Srivastava, K. R. Thomas, J. C. Dudda, K. D. Klonowski, and D. J. Campbell. 2014. CCR7 provides localized access to IL-2 and defines homeostatically distinct regulatory T cell subsets. *J Exp Med* 211: 121-136.
6. Luo, C. T., W. Liao, S. Dadi, A. Toure, and M. O. Li. 2016. Graded Foxo1 activity in Treg cells differentiates tumour immunity from spontaneous autoimmunity. *Nature* 529: 532-536.
7. Gratz, I. K., and D. J. Campbell. 2014. Organ-specific and memory treg cells: specificity, development, function, and maintenance. *Front Immunol* 5: 333.
8. Delacher, M., C. D. Imbusch, D. Weichenhan, A. Breiling, A. Hotz-Wagenblatt, U. Trager, A. C. Hofer, D. Kagebein, Q. Wang, F. Frauhammer, J. P. Mallm, K. Bauer, C. Herrmann, P. A. Lang, B. Brors, C. Plass, and M. Feuerer. 2017. Genome-wide DNA-methylation landscape defines specialization of regulatory T cells in tissues. *Nat Immunol* 18: 1160-1172.
9. Vasanthakumar, A., K. Moro, A. Xin, Y. Liao, R. Gloury, S. Kawamoto, S. Fagarasan, L. A. Mielke, S. Afshar-Sterle, S. L. Masters, S. Nakae, H. Saito, J. M. Wentworth, P. Li, W. Liao, W. J. Leonard, G. K. Smyth, W. Shi, S. L. Nutt, S. Koyasu, and A. Kallies. 2015. The transcriptional regulators IRF4, BATF and IL-33 orchestrate development and maintenance of adipose tissue-resident regulatory T cells. *Nat Immunol* 16: 276-285.
10. Wohlfert, E. A., J. R. Grainger, N. Bouladoux, J. E. Konkel, G. Oldenhove, C. H. Ribeiro, J. A. Hall, R. Yagi, S. Naik, R. Bhairavabhotla, W. E. Paul, R. Bosselut, G. Wei, K. Zhao, M. Oukka, J. Zhu, and Y. Belkaid. 2011. GATA3 controls Foxp3(+) regulatory T cell fate during inflammation in mice. *J Clin Invest* 121: 4503-4515.
11. Kee, B. L. 2009. E and ID proteins branch out. *Nat Rev Immunol* 9: 175-184.
12. Quong, M. W., W. J. Romanow, and C. Murre. 2002. E protein function in lymphocyte development. *Annu Rev Immunol* 20: 301-322.
13. Yang, C. Y., J. A. Best, J. Knell, E. Yang, A. D. Sheridan, A. K. Jesionek, H. S. Li, R. R. Rivera, K. C. Lind, L. M. D'Cruz, S. S. Watowich, C. Murre, and A. W. Goldrath. 2011. The transcriptional regulators Id2 and Id3 control the formation of distinct memory CD8+ T cell subsets. *Nat Immunol* 12: 1221-1229.
14. Omilusik, K. D., L. A. Shaw, and A. W. Goldrath. 2013. Remembering one's ID/E-ntity: E/ID protein regulation of T cell memory. *Curr Opin Immunol* 25: 660-666.
15. Miyazaki, M., R. R. Rivera, K. Miyazaki, Y. C. Lin, Y. Agata, and C. Murre. 2011. The opposing roles of the transcription factor E2A and its antagonist Id3 that orchestrate and enforce the naive fate of T cells. *Nat Immunol* 12: 992-1001.
16. Omilusik, K. D., M. S. Nadjsombati, L. A. Shaw, B. Yu, J. J. Milner, and A. W. Goldrath. 2018. Sustained Id2 regulation of E proteins is required for terminal differentiation of effector CD8(+) T cells. *J Exp Med* 215: 773-783.
17. Shaw, L. A., S. Belanger, K. D. Omilusik, S. Cho, J. P. Scott-Browne, J. P. Nance, J. Goulding, A. Lasorella, L. F. Lu, S. Crotty, and A. W. Goldrath. 2016. Id2 reinforces TH1 differentiation and inhibits E2A to repress TFH differentiation. *Nat Immunol* 17: 834-843.

18. Miyazaki, M., K. Miyazaki, S. Chen, M. Itoi, M. Miller, L. F. Lu, N. Varki, A. N. Chang, D. H. Broide, and C. Murre. 2014. Id2 and Id3 maintain the regulatory T cell pool to suppress inflammatory disease. *Nat Immunol* 15: 767-776.
19. Rauch, K. S., M. Hils, E. Lupar, S. Minguet, M. Sigvardsson, M. E. Rottenberg, A. Izcue, C. Schachtrup, and K. Schachtrup. 2016. Id3 Maintains Foxp3 Expression in Regulatory T Cells by Controlling a Transcriptional Network of E47, Spi-B, and SOCS3. *Cell Rep* 17: 2827-2836.
20. Rauch, K. S., M. Hils, A. J. Menner, M. Sigvardsson, S. Minguet, P. Aichele, C. Schachtrup, and K. Schachtrup. 2017. Regulatory T cells characterized by low Id3 expression are highly suppressive and accumulate during chronic infection. *Oncotarget* 8: 102835-102851.
21. Lee, J. H., S. G. Kang, and C. H. Kim. 2006. FoxP3+ T Cells Undergo Conventional First Switch to Lymphoid Tissue Homing Receptors in Thymus but Accelerated Second Switch to Nonlymphoid Tissue Homing Receptors in Secondary Lymphoid Tissues. *The Journal of Immunology* 178: 301-311.
22. Mackay, L. K., A. Rahimpour, J. Z. Ma, N. Collins, A. T. Stock, M. L. Hafon, J. Vega-Ramos, P. Lauzurica, S. N. Mueller, T. Stefanovic, D. C. Tscharke, W. R. Heath, M. Inouye, F. R. Carbone, and T. Gebhardt. 2013. The developmental pathway for CD103(+)CD8+ tissue-resident memory T cells of skin. *Nat Immunol* 14: 1294-1301.
23. Schenkel, J. M., and D. Masopust. 2014. Tissue-resident memory T cells. *Immunity* 41: 886-897.
24. Milner, J. J., C. Toma, B. Yu, K. Zhang, K. Omilusik, A. T. Phan, D. Wang, A. J. Getzler, T. Nguyen, S. Crotty, W. Wang, M. E. Pipkin, and A. W. Goldrath. 2017. Runx3 programs CD8(+) T cell residency in non-lymphoid tissues and tumours. *Nature* 552: 253-257.
25. Siede, J., A. Frohlich, A. Datsi, A. N. Hegazy, D. V. Varga, V. Holecska, H. Saito, S. Nakae, and M. Lohning. 2016. IL-33 Receptor-Expressing Regulatory T Cells Are Highly Activated, Th2 Biased and Suppress CD4 T Cell Proliferation through IL-10 and TGFbeta Release. *PLoS One* 11: e0161507.
26. Li, C., J. R. DiSpirito, D. Zemmour, R. G. Spallanzani, W. Kuswanto, C. Benoist, and D. Mathis. 2018. TCR Transgenic Mice Reveal Stepwise, Multi-site Acquisition of the Distinctive Fat-Treg Phenotype. *Cell*.
27. Arvey, A., J. van der Veeken, R. M. Samstein, Y. Feng, J. A. Stamatoyannopoulos, and A. Y. Rudensky. 2014. Inflammation-induced repression of chromatin bound by the transcription factor Foxp3 in regulatory T cells. *Nat Immunol* 15: 580-587.
28. Sun, I. H., M. H. Oh, L. Zhao, C. H. Patel, M. L. Arwood, W. Xu, A. J. Tam, R. L. Blosser, J. Wen, and J. D. Powell. 2018. mTOR Complex 1 Signaling Regulates the Generation and Function of Central and Effector Foxp3(+) Regulatory T Cells. *J Immunol*.
29. Couter, C. J., and N. K. Surana. 2016. Isolation and Flow Cytometric Characterization of Murine Small Intestinal Lymphocytes. *JoVE*: e54114.
30. Srivastava, S., M. A. Koch, M. Pepper, and D. J. Campbell. 2014. Type I interferons directly inhibit regulatory T cells to allow optimal antiviral T cell responses during acute LCMV infection. *J Exp Med* 211: 961-974.

Figure Legends

Figure 1: Id3 is dynamically expressed in T_R and regulated by TCR signaling

A) Representative flow cytometry plots of Id3-GFP and Foxp3-RFP expression by gated splenic TCRβ$^+$ CD4$^+$ T cells. B) Representative flow cytometry analysis of Id3-GFP expression by splenic CD44^{lo}CD62L^{hi} cT_R and CD44^{hi}CD62L^{lo} eT_R gated as indicated. (Bottom left) Graphical analysis of gMFI of Id3-GFP in each of the three gated T_R populations. C) Representative flow cytometry plots and graphical analysis of Id3-GFP expression by gated splenic TCRβ$^+$ CD4$^+$ Foxp3$^+$ T_R 48 hours after stimulation, summary of 2 independent expts. D) Representative flow cytometry plots and graphical analysis of CD44 and Id3-GFP expression by gated TCRβ$^+$CD4$^+$Foxp3$^+$ T_R recovered from the LNs of RAG1-deficient mice 2 weeks after transfer of the indicated T_R population, summary of 2 independent experiments, n=2-4 mice per group. Significance determined by one way ANOVA with Tukey's post-test for pairwise comparisons, *p <0.05, **p < 0.01, ****p < 0.001

Figure 2: Id3$^-$ eT_R express markers of activation and are more suppressive than Id3$^+$ T_R

A) Representative flow cytometry histograms and graphical analysis of expression of the indicated markers by gated splenic T_R populations. B) (Top) Representative flow cytometry analysis of CPD dilution by CD4$^+$Foxp3$^-$ effector T cells stimulated with or without the indicated T_R populations. (Bottom) Graphical analysis of suppression by each of the indicated populations, n=3. Significance determined by one way ANOVA with Tukey's post-test for pairwise comparisons, *p <0.05, **p < 0.01, ****p < 0.001

Figure 3: Id3$^+$ and Id3$^-$$T_R$ have distinct transcriptional profiles

A) PCA of RNA-seq data from LN and splenic Id3$^+$ cT_R, Id3$^+$ eT_R and Id3$^-$ eT_R populations sorted from three individual mice. B) Bar graphs showing the number of differentially expressed genes (adj.p.value < 0.05 and log2FC >1) for each of the indicated pairwise comparisons. C) Graphical analysis of normalized transcript reads for Id2 or Id3 from RNA-seq data. D) The 300 most differentially expressed genes (determined by F value) were split into the upregulated (red) and downregulated (blue) fractions based expression in Id3$^-$ eT_R vs Id3$^+$ cT_R. Graph shows the mean log2FC compared to Id3$^+$ cT_R for both eT_R populations. Error bars and shaded area represent 1x SD. E) Heatmap and hierarchical clustering of splenic RNA-seq samples based on the 300 most variably expressed genes. F) Heatmap and hierarchical clustering of splenic RNA-seq samples based on T_R signature genes identified in reference (9). G) GO term enrichment analysis for DE genes of Id3$^-$ eT_R vs. Id3$^+$ eT_R. Dashed lines represent adjusted p values of 0.05 and 0.01. H) Heatmap and hierarchical clustering of splenic RNA-seq samples based on DE genes found in the top 6 GO functional categories enriched in the comparison of Id3$^+$ and Id3$^-$ eT_R.

Figure 4: Id3$^-$ eT_R are enriched and resident in non-lymphoid tissues

A) Representative flow cytometry histograms and graphical analysis of expression of the CD69 and CD103 by gated splenic T_R populations. B) Enrichment of CD8$^+$ T_{RM} (red) or circulating T cell (blue) gene sets along ranked lists of the indicated pairwise comparisons. C) Heatmap and hierarchical clustering of splenic RNA-seq samples based on ST2$^+$ tissue T_R associated genes. D) Representative flow cytometry plots of CD103 and CD69 expression by gated TCRβ$^+$ CD4$^+$ Foxp3$^+$ T_R in the indicated tissues. E) Graphical analysis of Id3$^-$ eT_R frequency among total T_R in

various tissues. F) Representative histograms of GFP expression from various tissues of Id3-GFP x Foxp3-mRFP mice, gated on TCRβ$^+$ CD4$^+$ Foxp3$^+$ T_R.

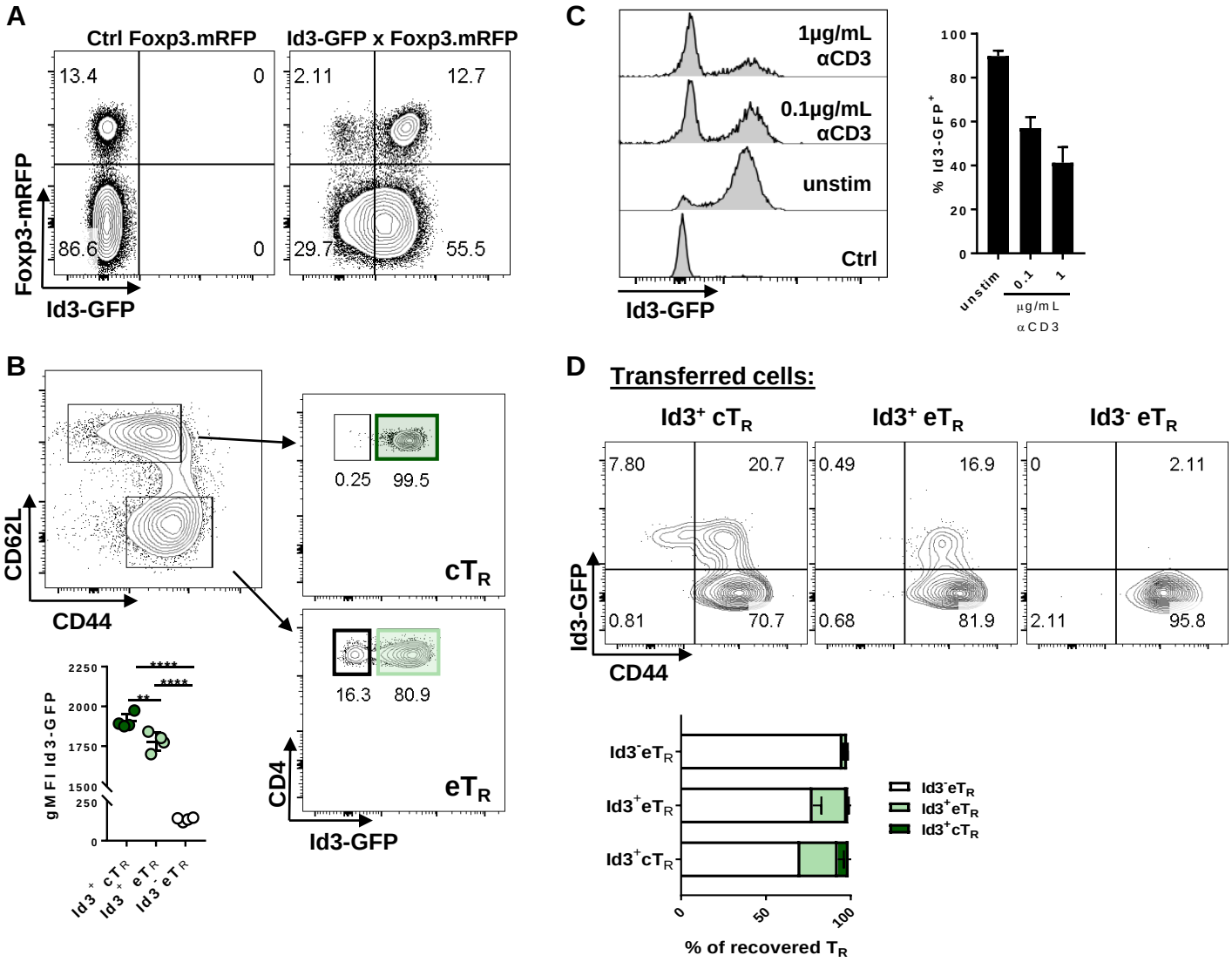

Id3 is dynamically expressed in T_R and regulated by TCR signaling

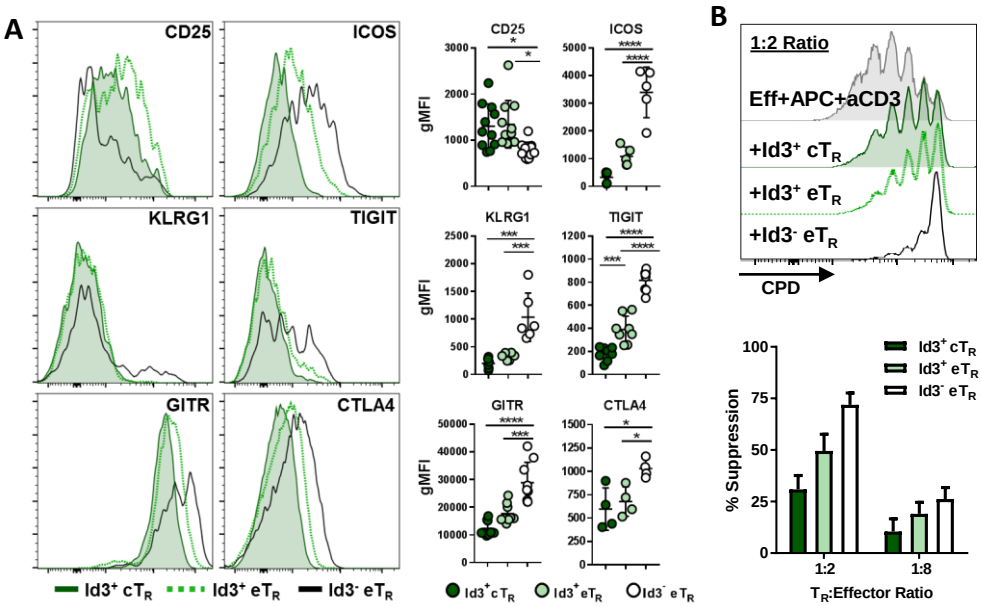

Id3$^-$ eT$_R$ express inhibitory markers and are highly suppressive

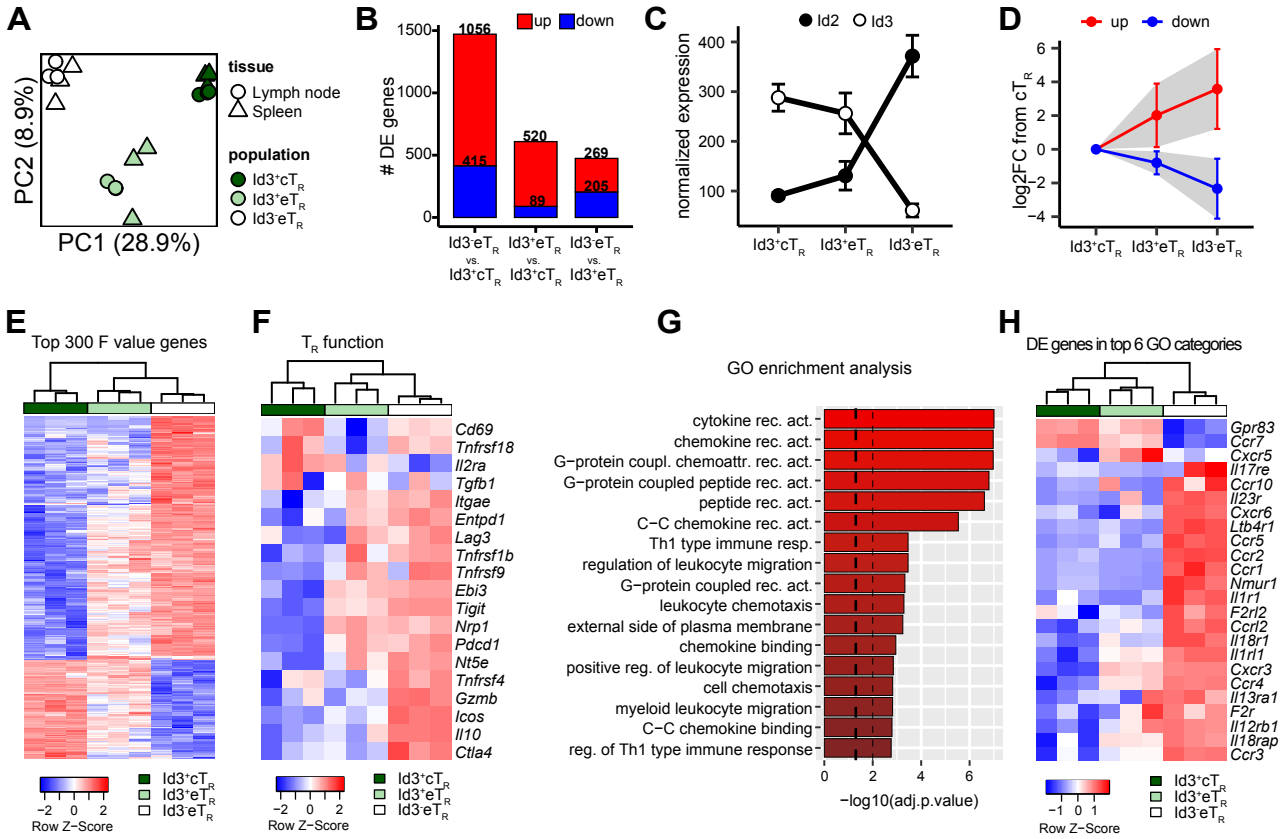

Transcriptional profiling highlights the stepwise differentiation of Id3$^-$ eT$_R$

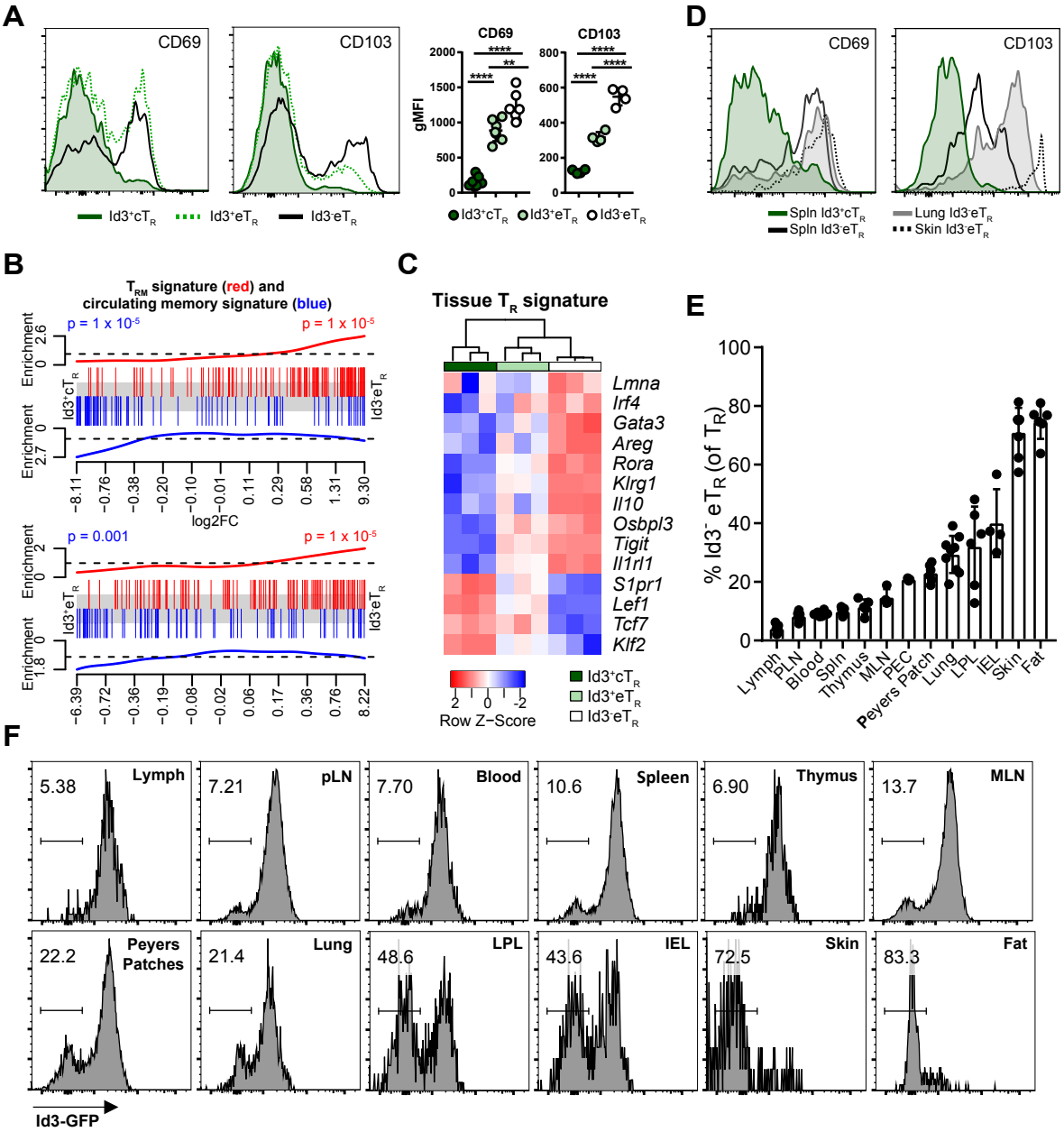

Transcriptional profiling highlights the stepwise differentiation of Id3$^-$eT$_R$